Appl. Phys. A (2016) 122:690
DOI 10.1007/s00339-016-0210-9

Applied Physics A
Materials Science & Processing

The effect of local fluence on the micropatterning of poly(ethylene terephthalate) foils through proton beam writing

C. T. de Souza[1] · E. M. Stori[1,2] · L. A. Boufleur[1] · R. M. Papaléo[3] · J. F. Dias[1]

Received: 13 January 2016 / Accepted: 9 June 2016 / Published online: 22 June 2016

Abstract In this work, we investigate the influence of ion fluence on the development of microstructures produced by 2.2 MeV H^+ impinging on 12-μm-thick poly(ethylene terephthalate) (PET, Mylar®) foils. Several lines of 1×100 pixels corresponding to approximately 2.5×101.5 μm^2 were patterned on PET foils using different ion fluences (from 10^{12} to 10^{17} H^+/cm^2) and etching times (from 1 to 60 min). We observe the presence of three different behaviors according to the ion fluence. Long etching times are necessary to open the structure in the low fluence regime, while moderate fluences require shorter etching times. In the high fluence regime, a more complex scenario emerges where short etching times lead to structures either fully or partially developed.

1 Introduction

Proton beam writing (PBW) is a direct lithographic technique that has gained attention in recent years due to the possibility of producing 3-D structures with high aspect ratio and spatial resolution without the use of lithographic masks [1–9]. In a recent review on this subject, van Kan et al. [10] have shown that regardless of the nature of the resist (positive or negative), parameters like ion fluence and etching procedure play a key role in the quality of the structures obtained through PWB. Among those materials used for micromachining purposes by PBW [10, 11] are SU-8 [4, 5, 7, 9], PMMA [1, 2, 6, 12–15], silicon [16], CR-39 [17] and silsesquioxane [18, 19]. The results presented by these reports show the importance of careful choice of ion fluence and etching procedure for each material under study [1, 2, 4–7, 9, 13, 14, 20–24].

Among several polymers, poly(ethylene terephthalate), better known as simply PET, finds several applications in membrane technology and biosensors [25]. Similarly to other polymers discussed above, patterning of PET through the PBW technique is expected to be strongly dependent on the type of ion, beam energy and ion fluence [26]. Indeed, the physical and chemical changes induced by the beam and the subsequent chemical etching of the exposed areas are directly linked to those parameters [22–24, 27–30]. In respect of the chemical treatment, the kinetics is highly complex and includes steps such as the transport and adsorption of etchant molecules by the polymer surface, chemical reactions of these molecules with the weaker bonds of the structure, the diffusion of reactional products and the final elimination of end-products of the reactions.

In this work we investigated the influence of the local fluence on the development of micropatterns produced by 2.2 MeV protons on poly(ethylene terephthalate) (PET, Mylar®) foils. The effects of ion fluence on the minimum time required for the removal of the exposed material and on the final dimensions and morphology of the patterned lines were evaluated. Possible mechanisms behind these effects were discussed.

✉ C. T. de Souza
clau_telles@yahoo.com.br

[1] Ion Implantation Laboratory, Institute of Physics, Federal University of Rio Grande do Sul, CP 15051, Porto Alegre, RS CEP 91501-970, Brazil

[2] Ion Beam Centre, Advanced Technology Institute, Faculty of Engineering and Physical Sciences, University of Surrey, Guildford, Surrey GU2 7XH, UK

[3] Faculty of Physics, Pontifical Catholic University of Rio Grande do Sul, Av. Ipiranga 6681, Porto Alegre, RS CEP 90619-900, Brazil

2 Experimental

The irradiations were performed with a 3 MV Tandetron accelerator equipped with an Oxford microprobe system operating in triplet mode. Poly(ethylene terephthalate) (PET, Mylar®) foils of 1 cm^2 and 12 μm thick were irradiated at room temperature with 2.2 MeV H^+. Such high energetic protons are transmitted through the foils since their penetration in Mylar is about 60 μm according to simulations carried out using the SRIM software [31]. Therefore, the polymer will be modified by the proton beam along its entire thickness. Finally, typical proton currents were in the range of 100–200 pA during the patterning of the foils.

The beam spot size was estimated using the profile of the beam across the edges of a 2000 mesh copper grid and was approximately 2.5 × 2.5 μm^2. Asymmetries of about 30 % in the *Y* direction (see definition of the coordinate system in Fig. 1) occurred in some irradiations. Lines of 1 × 100 pixels were patterned on the samples in steps of 1 μm using different number N_i of ions per pixel. N_i was varied from 1.25×10^5 H^+/pixel up to 4.7×10^9 H^+/pixel. The average fluences ϕ used to structure the lines were estimated as $\phi = 100\ N_i/A$, where *A* is the area of the irradiated line covering 100 pixels. The effective irradiated area was about 2.5 × 101.5 μm^2, which takes into account the beam spot size and neglects the tail of the beam profile where a small fraction of the ions is located. Thus, the estimated average fluences ϕ varied from 4.9×10^{12} H^+/cm^2 up to 1.8×10^{17} H^+/cm^2. However, as the beam spot was larger than the steps the ion probe moves from one pixel to the next, the writing procedure results in a non-uniform fluence profile along the line due to the superposition of the beam at particular positions. Figure 1 depicts a gross estimation of the fluence profile along a patterned line assuming an idealized squared beam spot of 2.5 × 2.5 μm^2 with sharp edges. The beam spot would exceed the pixel length by 0.75 μm at all sides. At the beginning and the end of the line, there is a region where the beam hits the polymer just once (labeled as region *S*) and no beam overlapping takes place. In the regions labeled D and T, the beam hits the polymer twice and three times, respectively. Overall, this effect gives rise to an indented fluence profile along the line (panel B of Fig. 1). The local fluences at regions S, D and T would be approximately 0.4, 0.8 and 1.2 ϕ, respectively.

In the estimations shown above, the actual shape of the microbeam (resembling a Gaussian curve with a somewhat flat peak) was not taken into account. Despite the number of ions in the tail of the beam profile peak is relatively small (about 15 %), they will also contribute to the fluence at neighboring pixels. Moreover, further spreading of the beam occurs due to lateral straggling of the ions. According to TRIM simulations [31], 2.2 MeV protons contribute with a lateral spreading of about 1 μm at the end of the 12-μm-thick PET foil. All these factors combined together (including the beam asymmetry in the *Y* direction) could lead to a smoothing of the idealized fluence profile shown in Fig. 1 and will contribute to the enlargement of the region modified by the beam.

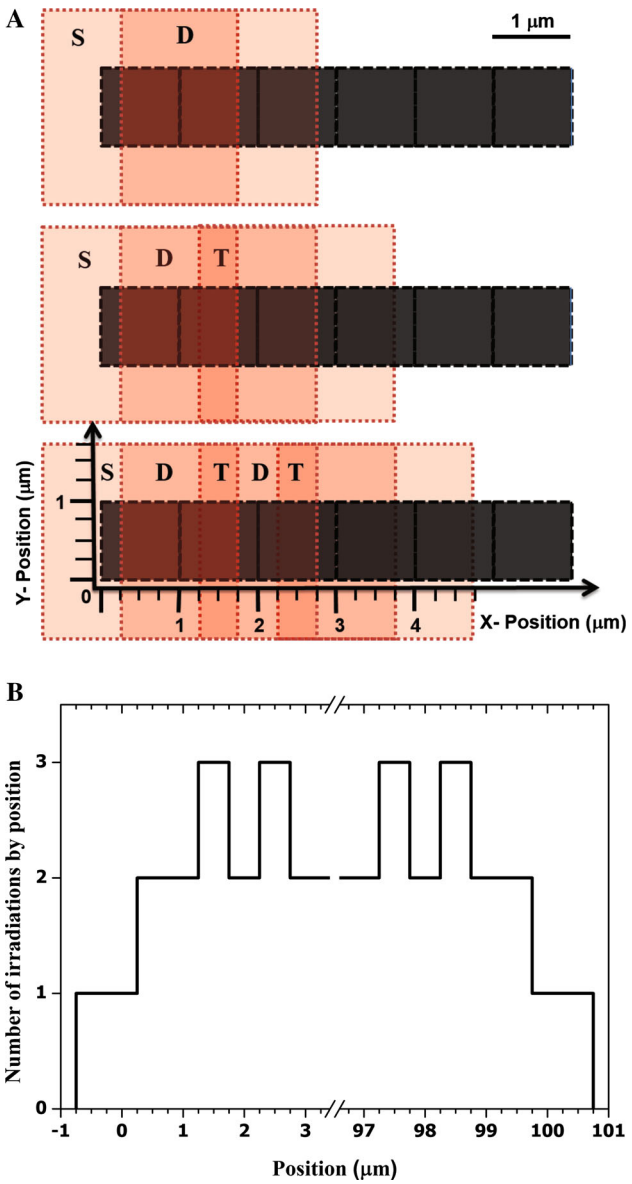

Fig. 1 **a** Schematic drawing of the patterning process of 1 *line* with a pixel size equal to 1 × 1 μm^2 (*dark squares*) with a beam of 2.5 × 2.5 μm^2 (*red squares*). At the beginning and the end of the structure, there is no overlap of the beam (*region S*). Regions characterized by one and two overlaps of the beam are labeled as *D* and *T*, respectively. **b** Number of times the beam hits the sample as function of the beam position

Although the proton irradiation modifies the chemical structure of PET, it removes very little material as sputtering is very inefficient for protons of this energy. Therefore, there is no formation of holes in the polymer through the direct action of the beam. In order to develop the patterned lines into holes, the samples were submitted to a chemical attack. In short, the irradiated samples were etched with a 6 M NaOH solution in a thermal bath at (60 ± 1) °C with continuous magnetic agitation. The etching time varied from 2 up to 60 min for each fluence. Imaging of the samples was carried out using a scanning electron microscope model EVO MA-10 ZEISS® in the secondary electron mode and with an acceleration voltage of 12 kV. All samples were coated with gold in order to avoid charge buildup during the measurements. The images were obtained in plane-view mode and analyzed using the ImageJ® software. The width and length of the patterned lines were measured from profiles drawn across both horizontal directions. The edges of the profiles were fitted with error functions in order to obtain the desired dimensions [32].

3 Results and discussions

Once the irradiated polymer is immersed in the chemical solution for the etching procedure, both irradiated and non-irradiated portions of the polymer interact with the etchant. Non-irradiated areas take much longer to be corroded by the etchant. The thickness of the non-irradiated PET foil decreases at a rate of approximately 0.10 μm per min of chemical attack [33, 34]. Once the structure is developed by the chemical attack, the etchant interacts with the inner walls of the structure, thus affecting their roughness. Angled SEM images [32] revealed that etching times up to 20 min yield relatively smooth walls. As the etching time increases, the roughness of the walls degrades progressively.

During selective etching, the removal process does not start immediately after the immersion of the polymer into the etching solution but only after a certain induction time. The opening time is defined as the shortest etching time required to remove all the material modified by the proton beam. Figure 2 shows the opening times as a function of the average fluence of the proton beam. The uncertainties shown in this figure represent the time difference between the opening time and the maximum etching time tested for which the opening does not occur. The data can be sorted out in three distinct regions labeled as I, II and III according to the different behavior found for the micropatterning process.

For fluences smaller than $\sim 5 \times 10^{15}$ H^+/cm^2 (Region I), relatively long opening times were found. Etching times

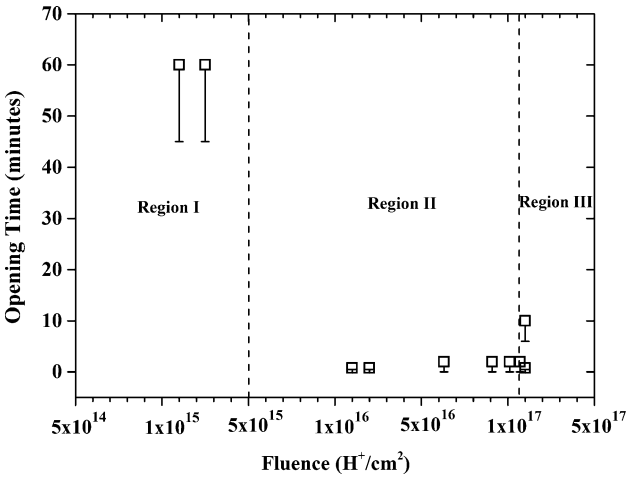

Fig. 2 Opening time of the structures as a function of the ion fluence. *Regions I*, *II* and *III* refer to low, medium and high fluences. See text for further details

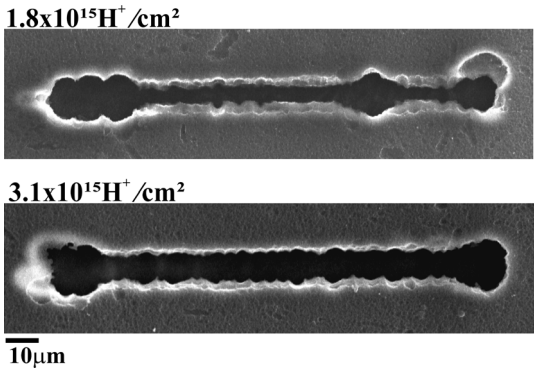

Fig. 3 SEM images of PET foils depicting lines patterned with low fluences (corresponding to Region I of Fig. 2) and etched during 60 min

of the order of 60 min are required to remove the activated area by the beam for fluences around 1×10^{15} H^+/cm^2. Below that level of fluence (tested from 3.1×10^{14} H^+/cm^2 down to 4.9×10^{12} H^+/cm^2), full opening was not achieved even at the longest etching time used in this work. This is expected because to develop the patterned structure, the reaction rate in the irradiated zone has to be larger then the etching rate of the unmodified material [35]. At very low fluences, the small number of scissions induced by the beam in the PET chains makes preferential etching in the bombarded areas less efficient [36]. Figure 3 shows the SEM images obtained for the lines irradiated with low fluences (1.8×10^{15} and 3.1×10^{15} H^+/cm^2) after 60 min of etching, thus corresponding to Region I of Fig. 2. The lines are characterized by an irregular shape with indented borders. Moreover, it can be observed signs of corrosion even in the non-irradiated portion of the polymer, which reflects the relatively long time the polymer has been exposed to the etchant.

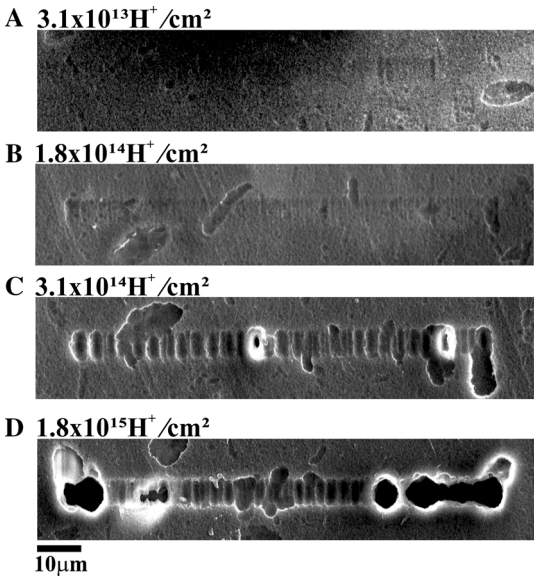

Fig. 4 SEM images of PET foils depicting lines patterned with different fluences and etched during 45 min. *Panel A* 3.1×10^{13} H^+/cm^2; *panel B* 1.8×10^{14} H^+/cm^2; *panel C* 3.1×10^{14} H^+/cm^2; and *panel D* 1.8×10^{15} H^+/cm^2

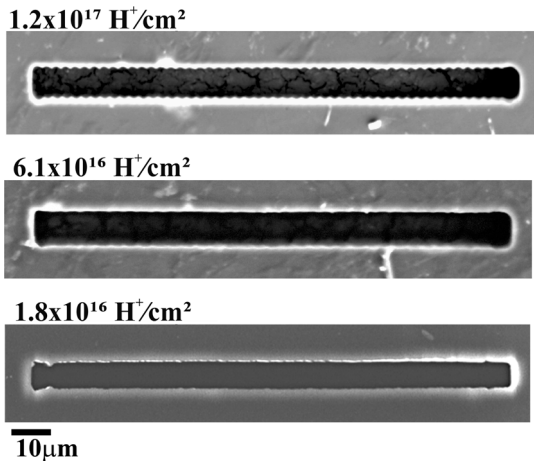

Fig. 5 SEM images of PET foils depicting lines patterned with moderate fluences (corresponding to Region II of Fig. 2) and etched during 2 min

It is also interesting to see the morphology of the patterned lines for etching times smaller than the opening time. Figure 4 depicts microstructures obtained after 45 min of chemical attack and fluences ranging from 3.1×10^{13} H^+/cm^2 up to 1.8×10^{15} H^+/cm^2. At the lowest fluences (panels A and B), the SEM images reveal faint spots corresponding to the region scanned by the proton beam. On the other hand, at slightly larger fluences (panels C and D), a clear pattern of rectangular cavities along the line can be observed. This pattern indicates a complex fluence profile during the irradiations. Effects like those discussed in Fig. 1 could be responsible for the observed structures. Fluctuations in the beam intensity during the irradiations could play a role as well. In this regime, it seems that the etching rate is very sensitive to the ion fluence, and a non-uniform irradiation would be enough to change substantially the etching rate and result in a non-uniform pattern. Moreover, fully developed regions start to show up in panels C and D.

Much shorter etching times are required in order to fully develop the structures when moderate-to-high fluences (corresponding to Region II of Fig. 2) are employed. In this case, at most 2 min of etching is sufficient for the complete removal of material from the interior of the structure. Moreover, the lines have a well-defined rectangular shape with smooth borders. This is seen in Fig. 5 which shows SEM images for lines structured with fluences of 1.8×10^{16}, 6.1×10^{16} and 1.2×10^{17} H^+/cm^2. Therefore, fluences in the range of those shown in Region II of Fig. 2 coupled to shorter etching times correspond to the optimum conditions for the PBW technique as far as thin PET foils are concerned.

At even higher fluences (corresponding to Region III of Fig. 2), a different behavior was found. Etched lines were expected to be well defined for etching times close to the opening time found for structures located in Region II of Fig. 2, i.e., 2 min. Indeed, panel A of Fig. 6 proves that that is the case. While 6 min of etching time still yields quite reasonable results (panel B of Fig. 6), longer etching times tend to deteriorate the structure (panel C of Fig. 6). However, the opening times for such high fluence, i.e., 1.8×10^{17} H^+/cm^2, were not always reproducible. For some samples irradiated with the same fluence, large portions of wormlike-shaped material were still attached to the PET substrate (panels D, E and F of Fig. 6) for etching times as long as 45 min. The irradiated areas were not dissolved by the etchant, but only detached along different portions of the line wall. One can also observe that for very long etching times (panels C and F), the walls are porous, showing a high degree of degradation, most probably due to defects in the foils that are amplified by the etching procedure.

The formation of such etching-resistant blocks can be explained by the extensive rearrangement and crosslinking of the PET chains induced by the proton beam. Although ion irradiation of PET induces both scission and crosslinking events [37, 38], different authors have reported the predominance of crosslinking in PET and other polymeric substrates at high ion fluences [36, 39]. The reduction in solubility of the modified material occurs due to the increase in the molecular weight of the chains or the formation of a carbon-rich crosslinked network. This kind of behavior allows PET to change from a positive to a negative resist [10, 40].

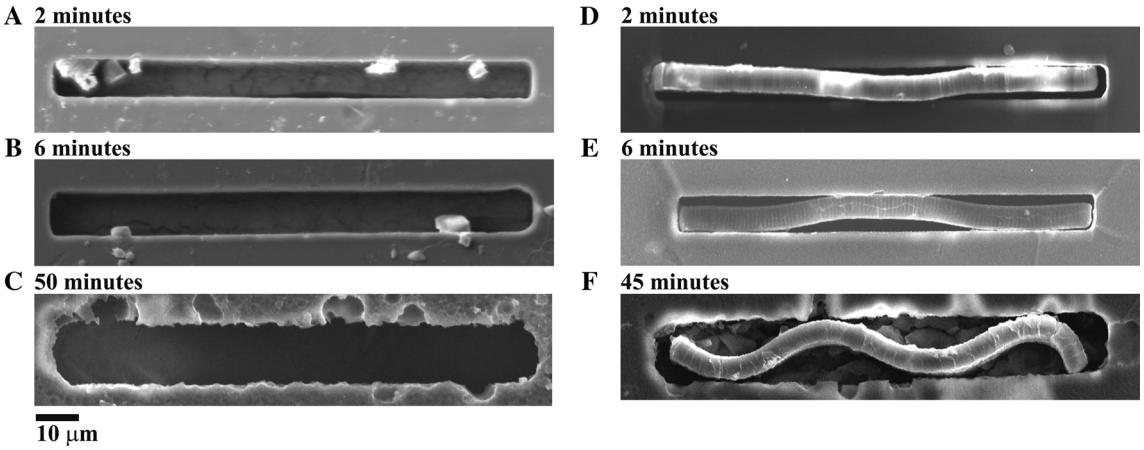

Fig. 6 SEM images of PET foils depicting lines patterned with 1.8×10^{17} H^+/cm^2 and etched during different times: 2 (*panels A* and *D*); 6 (*panels B* and *E*); 45 (*panel F*); and 50 min (*panel C*)

The edges of the irradiated lines are characterized by an interface region of decreasing fluence from inside to outside the structure, probably due to the Gaussian shape of the ion beam. At this interface, scission is still predominant, facilitating the removal of the irradiated material by detachment. The variability of the etching time needed to fully detach the blocks formed inside the structure can be attributed to the random distribution of connecting points where the irradiated area is kept chemically bound to the non-irradiated material.

4 Concluding remarks

In this work we investigated the influence of ion fluence on the development of micropatterns produced by 2.2 MeV H^+ impinging on PET foils. We identified three different fluence regimes associated with the micropatterning process. At low fluences, long etching times are required for the structures to be developed. Moreover, the lines produced in this regime are quite irregular. In this regime, the removal process is hampered by the low level of scissions induced by the proton beam in the polymer. At moderate fluences, short etching times are required and high-quality patterning is produced. At high fluences, crosslinking plays an important role with severe consequences for the chemical attack. As a result, the removal of material was neither always efficient nor reproducible, leading to relatively poor quality structures. The randomness of this process was attributed to the existence of connecting points where the irradiated area is kept chemically bound to the non-radiated material. Finally, it is worth mentioning that the boundaries set for the ion fluences discussed here may change if different etching conditions are employed such as temperature and concentration of the etchant. However, the general trend seen here is expected to be the same, namely regimes of low, medium and high fluences with different kinetics of material removal and specific morphologies for the patterned lines.

As far as PBW is concerned, the size of the beam spot and the pixel size must be considered in the patterning of polymers like PET. If a perfect match between these two dimensions is not achieved, then overlaps or gaps may lead to an uneven fluence across the irradiated region, thus impacting on the characteristics of the final structure.

The results obtained here will certainly contribute to foster the use of PET in the technology where microstructures are needed. For instance, electroactive polymers have attracted a lot of attention in the past years. Electroactive polymers patterned into precise microstructures can control the migration of ions in different ways. The present study shed some light on what are the best parameters for micropatterning such polymer.

Acknowledgments The authors acknowledge the financial support of the Brazilian agencies CAPES, CNPQ and FAPERGS.

References

1. S.Y. Chiam, J.A. van Kan, T. Osipowicz, C.N.B. Udalagama, F. Watt, Nucl. Instrum. Methods Phys. Res. B **260**(1), 455 (2007)
2. J.A. van Kan, A.A. Bettiol, B.S. Wee, T.C. Sum, S.M. Tang, F. Watt, Sens. Actuators A Phys. **92**(1–3), 370 (2001)
3. C. Acikgoza, M.A. Hempenius, J. Huskens, Eur. Polym. J. **47**(11), 2033 (2011)
4. C. Yang, A.A. Bettiol, Y. Shi, M. Bosman, H.R. Tan, W.P. Goh, J.H. Teng, E.J. Teo, Nucl. Instrum. Methods Phys. Res. B **306**, 281 (2013)
5. A.A. Bettiol, S.P. Turaga, Y. Yan, S.K. Vanga, S.Y. Chiam, Nucl. Instrum. Methods Phys. Res. B **306**, 271 (2013)
6. P.G. Shao, J.A. van Kan, K. Ansari, A.A. Bettiol, F. Watt, Nucl. Instrum. Methods Phys. Res. B **260**(1), 479 (2007)
7. T.C. Sum, A.A. Bettiol, J.A. van Kan, F. Watt, Appl. Phys. Lett. **83**(9), 1707 (2003)

8. F. Zhang, J.A. van Kan, S.Y. Chiam, F. Watt, Nucl. Instrum. Methods Phys. Res. B **260**, 474 (2007)
9. V.S. Kumar, S.P. Turaga, E.J. Teo, A.A. Bettiol et al., Microelectron. Eng. **102**, 33 (2013)
10. J.A. van Kan, P. Malar, Y.H. Wang, Appl. Surf. Sci. **310**, 100 (2014)
11. F. Watt, M.B.H. Breese, A.A. Bettiol, J.A. van Kan, Mater. Today **6**, 20 (2007)
12. R. Norarat, H.J. Whitlow, M. Ren, T. Osipowicz, J.A. van Kan, J. Timonen, F. Watt, Microelectron. Eng. **102**, 22 (2013)
13. Y.S. Ow, M.B.H. Breese, A.A. Bettiol, Nucl. Instrum. Methods Phys. Res. B **267**(12–13), 2289 (2009)
14. R. Huszank, S.Z. Szilasi, K. Vad, I. Rajta, Nucl. Instrum. Methods Phys. Res. B **267**(12–13), 2299 (2009)
15. S. Bolhuis, J.A. van Kan, F. Watt, Nucl. Instrum. Methods Phys. Res. B **267**, 2302 (2009)
16. E.J. Teo, M.H. Liu, M.B.H. Breese, E.P. Tavernier, A.A. Bettiol, D.J. Blackwood, F. Watt, Technol. Micro Opt. Nano Opt. II **5347**, 264 (2004)
17. J.A. van Kan, A.A. Bettiol, S.Y. Chiam, M.S.M. Saifullah, K.R.V. Subramanian, M.E. Welland, F. Watt, Nucl. Instrum. Methods Phys. Res. B **260**(1), 460 (2007)
18. J.A. van Kan, F. Zhang, C. Zhang, A.A. Bettiol, F. Watt, Nucl. Instrum. Methods Phys. Res. B **266**, 1676 (2008)
19. J.A. van Kan, A.A. Bettiol, F. Watt, Nano Lett. **6**, 579 (2006)
20. D. Mangaiyarkarasi, M.B.H. Breese, O.Y. Sheng, D.J. Blackwood, Nucl. Instrum. Methods Phys. Res. B **260**(1), 445 (2007)
21. G.A. Glass, A.D. Dymnikov, B. Rout, D.P. Zachry, Nucl. Instrum. Methods Phys. Res. B **260**(1), 372 (2007)
22. P. Mistry, I. Gomez-Morilla, G.W. Grime, R. Webb, C. Jeynes, R. Gwilliam, A. Cansell, M. Merchant, K.J. Kirkby, Nucl. Instrum. Methods Phys. Res. B **231**(1–4), 428 (2005)
23. J.A. van Kan, P. Malar, A.B. de Vera, X. Chen, A.A. Bettiol, F. Watt, Nucl. Instrum. Methods Phys. Res. A **645**(1), 113 (2011)
24. Y.H. Wang, P. Malar, J. Zhao, J.A. van Kan, Nucl. Instrum. Methods Phys. Res. B **260**(1), 419 (2007)
25. M. Ulbricht, Polymer **47**(7), 2217 (2006)
26. M. Abdesselam, D. Muller, M. Djebara, S. Ouichaoui, A.C. Chami, Nucl. Instrum. Methods Phys. Res. B **307**, 635 (2013)
27. E. Reichmanis, J.H. O'Donnell, *The effects of radiation on high-technology polymers* (ACS, Washington, DC, 1989), p. 381
28. J.P. Duraud, A. Le Moël, Nucl. Instrum. Methods Phys. Res. B **105**, 71 (1995)
29. J. Davenas, I. Stevenson, N. Celette, S. Cambon, J.L. Gardette, A. Rivaton, L. Vignouds, Nucl. Instrum. Methods Phys. Res. B **191**, 563 (2002)
30. L. Calcagno, G. Compagnini, G. Foti, Nucl. Instrum. Methods Phys. Res. B **65**, 413 (1992)
31. J.F. Ziegler, J.B. Biersack, M.D. Ziegler, The Stopping and Range of Ions in Matter, 15th edn (2015). Software available at www.srim.org
32. E.M. Stori, C.T. de Souza, L. Amaral, D. Fink, R.M. Papaléo, J.F. Dias, Nucl. Instrum. Methods Phys. Res. B **306**, 99 (2013)
33. C.T. Souza, E.M. Stori, D. Fink, V. Vacík, V. Svorck, R.M. Papaléo, L. Amaral, J.F. Dias, Nucl. Instrum. Methods Phys. Res. B **306**, 222 (2013)
34. E.M. Stori, C.T. Souza, J.F. Dias, J. Appl. Polym. Sci. **133**, 43253 (2016). doi:10.1002/APP.43253
35. D. Fink, *Transport Processes in Ion-Irradiated Polymers* (Springer, Berlin Heidelberg, Berlin, 2004), p. 337
36. W.L. Brown, Nucl. Instrum. Methods Phys. Res. B **37**, 270 (1989)
37. R. Spohr, et al. European Research Training Network EuNITT. 1 (2001)
38. P. Apel, Nucl. Instrum. Methods Phys. Res. B **208**, 11 (2003)
39. R.S. Thomaz, C.T. de Souza, R.M. Papaléo, Appl. Phys. A **104**(4), 1223 (2011)
40. T.M. Hall, J. Appl. Phys. **53**(6), 3997 (1982)